Spectroscopy in an extremely thin vapor cell: Comparing the cell-length dependence in fluorescence and in absorption techniques

D. Sarkisyan,* T. Varzhapetyan, A. Sarkisyan, Yu. Malakyan, and A. Papoyan
Institute for Physical Research, NAS of Armenia, Ashtarak-2, 378410 Armenia

A. Lezama
Instituto de Fisica, Facultad de Ingenieria, C.P. 30, Montevideo, Uruguay

D. Bloch and M. Ducloy
Labaratoire de Physique des Lasers, UMR 7538 du CNRS, Université Paris 13, F-93430 Villetaneuse, France
(Received 12 December 2003; revised manuscript received 26 March 2004; published 25 June 2004)

We compare the behavior of absorption and of resonance fluorescence spectra in an extremely thin Rb vapor cell as a function of the ratio of L/λ, with L the cell thickness ($L \sim 150-1800$ nm) and λ the wavelength of the Rb D_2 line ($\lambda = 780$ mn). The Dicke-type coherent narrowing [G. Dutier *et al.*, Europhys. Lett. **63**, 35 (2003)] is observed only in transmission measurements, in the linear regime, with its typical collapse and revival, which reaches a maximum for $L=(2n+1)\lambda/2$ (n integer). It is shown not to appear in fluorescence, whose behavior-amplitude, and spectral width, is more monotonic with L. Conversely, at high-intensity, the sub-Doppler saturation effects are shown to be the most visible in transmission around $L=n\lambda$.

DOI: 10.1103/PhysRevA.69.065802 PACS number(s): 42.50.Gy, 32.70.Jz, 42.62.Fi, 42.50.Md

Transmission spectroscopy in a thin cell of dilute vapor has been demonstrated as a sub-Doppler laser spectroscopy method [1–7]. The sub-Doppler features in a thin cell are caused by the fact that the duration of the atom-laser radiation interaction, governed by wall-to-wall trajectories, is anisotropic: the contribution of atoms with slow normal velocity is enhanced thanks to their longer interaction time with the laser field. Under normal incidence irradiation, the resonance of these atoms, flying nearly parallel to the wall and yielding a stronger contribution to the signal, appears to be insensitive to the Doppler shift. Recently, a series of extremely thin cells (ETC) of alkali-metal vapor, with the thickness L of the vapor column in the range 100 nm $< L < 1$ μm, have been developed [8]. The ETC allows one to obtain directly (without applying a frequency modulation technique) narrow sub-Doppler absorption and fluorescence spectra. Also, it has been demonstrated that for these ETCs, the fluorescence emission corresponds to a narrow resonant process. Recently, the ETC length dependence of the transmission signal has been analyzed, and the coherent Dicke-narrowing demonstrated in the optical domain [9]. It is the purpose of this report to compare the transmission and the fluorescence behaviors with respect to the cell length.

Among the factors that can influence the shape and magnitude of the transmission and fluorescence spectra of a thin vapor column confined in an ETC and make them sensitive to the cell length [9], one should notably take into account the transient behavior of the atomic absorption, which enhances the slow atom contribution, and the coherent response of the atomic dipole, that induces a maximal narrow contribution around $L=(2n+1)\lambda/2$ (where λ is the laser wavelength resonant with atomic transition) known as the coherent Dicke narrowing [2,9,10]. The Fabry-Perot (FP) nature of the ETC [11] tends to mix-up absorptive and dispersive responses, while the van der Waals atom-surface interaction contribution remains negligible for thickness $L > 200$ nm [12].

To achieve the smoothly variable L/λ value of the ETC, a new method involving thickness tuning by controlled external air pressure has been implemented (for details, see [13]). The design of the ETC itself is eventually similar to the one presented in [8]. The gap thickness measurement method with an accuracy of ~ 10 nm is described in [9]. For all the experiments, the temperature of the sidearm (T_{sa}) of the ETC was kept at $\sim 120\,^{\circ}$C (windows were overheated by 10°–15°), and this provides ^{87}Rb vapor density of $N \sim 6 \times 10^{12}$ at/cm^3. This value of the density has been derived from the Tailor-Langmuir equation and was justified by comparing low intensity peak absorption values in the ETC and in a room-temperature 1-cm-long Rb cell.

The studies were essentially performed with a 1 mm diameter beam issued from a $\lambda = 780$ nm, 25 MHz linewidth single-frequency cw laser diode, resonant for the D_2 line of ^{87}Rb. The beam was directed at normal incidence onto the ETC located inside the vacuum chamber, and the behavior was compared between a nonsaturating laser intensity of 0.4 mW/cm^2 and a larger intensity 20 mW/cm^2, susceptible to induce saturation effects when the cell length is sufficient [1]. The fluorescence spectra were detected by a photodiode with an aperture of 1 cm^2 placed at 90° from the laser radiation direction [14].

Figure 1 presents the line shape and magnitude of the resonant absorption, for various L values, either at a low intensity [Fig. 1(a): 0.4 mW/cm^2], or at a much higher intensity [Fig. 1(b): 20 mW/cm^2]. These absorption graphs have been normalized directly to the transmitted off-resonance pump intensity in order to remove most of the Fabry-Perot effects (actually, for length values that are not a multiple of $\lambda/2$, the absorption remains mixed up with some

*Corresponding author. FAX: 00374-32-31172; electronic address: david@ipr.sci.am

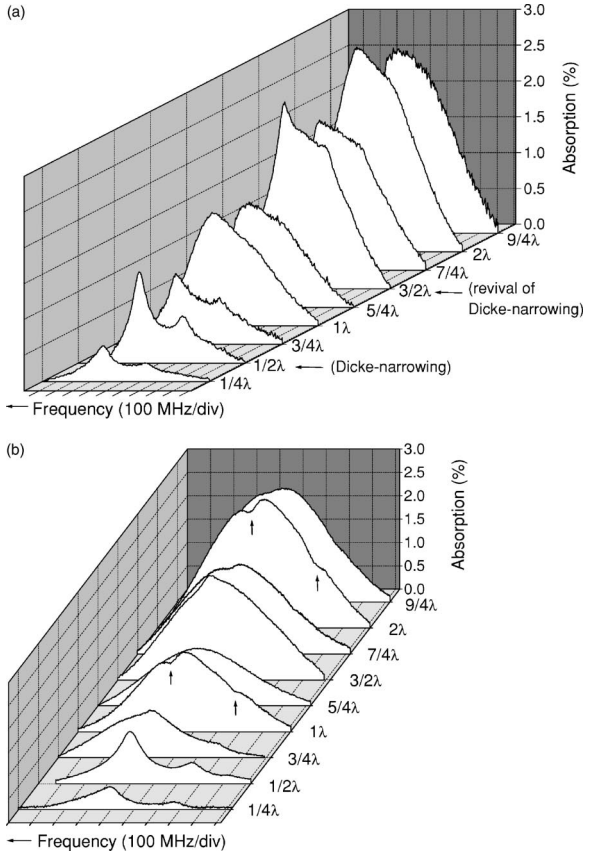

FIG. 1. The line shape and magnitude (in percents) of the absorption obtained with a step of L equal to $\lambda/4$ (L is increasing up to $9\lambda/4$) for the $^{87}\mathrm{Rb}\,D_2$ line, transitions $F_g=2\rightarrow F_e=1,2,3$, T_{sa} is $\sim 120\,^{\circ}\mathrm{C}$. (a) Laser intensity is $I=0.4\ \mathrm{mW/cm^2}$. The narrowest linewidth of the absorption is achieved for $L=\lambda/2$. The effect of collapse and revival of Dicke-type coherent narrowing is well seen. Although the effects of the FP nature of the ETC have been compensated for, an oscillating behavior of the absorption magnitude is clearly seen, with a λ periodicity. (b) Laser intensity $I=20\ \mathrm{mW/cm^2}$. For $L=\lambda$ and 2λ, the sub-Doppler dips of a reduced absorption are observable with a good contrast. These dips are caused by the fact that atoms flying nearly parallel to the windows undergo velocity selective saturation effects.

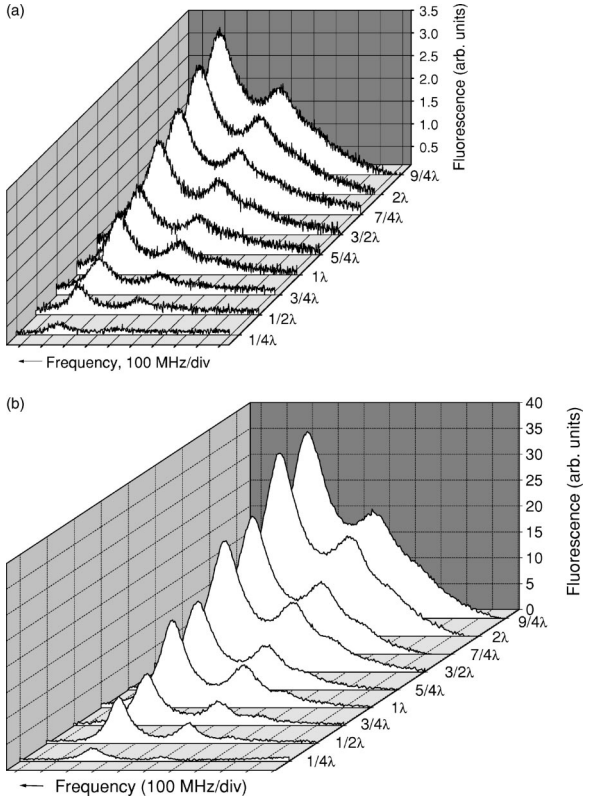

FIG. 2. The line shape and the magnitude of the resonant fluorescence obtained with a step of L equal to $\lambda/4$ (L is increasing up to $9\lambda/4$). Pump intensity I is (a) $0.4\ \mathrm{mW/cm^2}$ and (b) $20\ \mathrm{mW/cm^2}$.

dispersive behaviors [11]). In the low-intensity regime [Fig. 1(a)], there is clearly a length ($L=\lambda/2$) which produces the absorption spectrum with the narrowest linewidth. As already demonstrated in [9], this effect is the signature of the coherent Dicke-type narrowing, whose revival for $L=3\lambda/2$ is here more visible than in the original demonstration, in a cell whose thickness was limited to $L=10.5\lambda/8$. In contrast, for $L=\lambda$, there is no longer such a coherent narrowing, and the Doppler broadening affecting the transmission line shapes makes the hyperfine structure unresolved. Note that, as expected from the relaxation of the coherent buildup responsible for the Dicke narrowing [2], the oscillating character of the Dicke narrowing with the cell thickness vanishes for large thickness L: the narrow contribution tends to an asymptotic (L-independent) value, which is half of its value at $L=\lambda/2$, and its relative contrast decreases with respect to the broad pedestal which increases proportionally to the cell size. This explains the residual sub-Doppler contribution at $L=2\lambda$, in contrast to the $L=\lambda$ result. Accompanying these oscillations in the linewidth, one notes a correlated oscillation in the absorption amplitudes. These general features, associated with a linear coherent behavior, are not seen as sharply in Fig. 1(b), when the irradiating intensity is increased to $20\ \mathrm{mW/cm^2}$. Indeed, the Dicke-type narrowing originates in a coherent response at first-order, and is hence minored when high-order saturation effects take place. Also, one knows that, at high pump intensity, velocity-selective optical pumping or saturation can induce narrow sub-Doppler dips of reduced absorption as observed earlier [1] (observation had been performed both in direct transmission, and through a frequency modulation technique enabling an enhanced sensitivity [1–3]). Here, such narrow dips of reduced absorption are clearly observable for $L=\lambda$ and for $L=2\lambda$. This is essentially due to the fact that these contributions, that are intrinsically narrow, are the most visible on a broad background, when this narrow signature does not need to superimpose over the also narrow coherent Dicke-type response, that remains partly visible.

Figure 2 shows the line shape and magnitude of the resonant fluorescence in conditions (cell length, laser intensity) analogous to those of Fig. 1. The narrowest linewidth of the fluorescence spectra is obtained when L is in the range $\lambda/4<L\leqslant\lambda/2$ [in Fig. 1(a), we get 80 MHz (full width at half maximum), and optimal conditions—notably a smaller Rb density—would permit us to reach smaller linewidths [15]]. Note that in contrast to the transmission spectra, when

L increases, the linewidth of the fluorescence spectra increases monotonically, without oscillations of the linewidth versus L, while remaining below the Doppler broadening in all of our experimental conditions, including $L=9\lambda/4$. Note also that the fluorescence magnitudes [8] smoothly increase with L once the Fabry-Perot behavior of the ETC—with its $\lambda/2$ periodicity—is taken into account. Moreover, as an additional difference with the transmission spectra, there is no essential changes in the lineshapes behavior in the high-intensity regime [Fig. 2(b)], but for a small additional power broadening of the linewidths.

At last, it is worth pointing out that in these detailed studies of the behavior as a function of the cell length, the absorption spectrum remains always broader than the one observed in fluorescence (in our presented spectra, for the low-intensity regime, the minimal width for the absorption is 140 MHz—obtained at $L=\lambda/2$—vs 80 MHz for the fluorescence spectrum). This confirms one of our preliminary observations [8], although obtained at a time when the cell thickness parameter had not been considered. This general result must be related with the larger time needed to observe fluorescence, which implies both an absorption cycle and an emission process, inducing a narrower velocity selection, while the interferometric dependence of the coherent Dicke effect vanishes.

As illustrated below, these results are in good agreement with the theoretical modeling. For transmission spectra, in the absence of saturation, a complete (and analytical) theory had been given in [11]. For fluorescence, or to take into account the saturation effects in transmission spectroscopy, additional theoretical developments have been performed that will be reported elsewhere [16]. In this theory, the absorption and fluorescence spectra have been calculated in all orders of a pump field by means of numerical integration of the density matrix equation. Also, the real configuration for the D_2 line of Rb atoms has been taken into account [16]. We provide in Figs. 3 and 4 the numerical simulations obtained, respectively, for transmission and fluorescence, with the parameters corresponding to the $F_g=2\rightarrow F_e=1,2,3$ transitions of the ^{87}Rb D_2 line, and taking into account a laser linewidth $\Gamma_L\sim 3.5\gamma$, with $\gamma\approx 6$ MHz the spontaneous decay rate. We assume that the effective pump intensity is lower by a ratio of Γ_L/γ and thus, for the intensities 0.4 and 20 mW/cm^2 we use for the numerical simulations Rabi frequencies $\Omega=0.2\gamma$ and 1.5γ, correspondingly. Since the physical origin of the observed behavior is not clearly evident from this numerical model, we present below a qualitative optical Bloch vector illustration of the processes involved.

As is well known, the atomic response of a two-level atom (with $|g\rangle$ the ground state and $|e\rangle$ the excited state) can be calculated through the evolution of an optical Bloch vector $\mathbf{S}=(S_x,S_y,S_z)$, where $S_x=(\sigma_{eg}+\sigma_{ge})$, $S_y=i(\sigma_{eg}-\sigma_{ge})$, $S_z=(\sigma_{ee}-\sigma_{gg})$, and where σ_{ij}, stands for the components of σ, the density matrix of the atomic system in the rotating frame. Hence the absorption and fluorescence rate properties of a given two-level medium, respectively, depend on S_y and on $(1+S_z)$. The Bloch vector is known to precess around the pseudomagnetic field $\mathbf{B}=(\Omega,0,\delta)$, where Ω is the Rabi frequency, and δ the frequency detuning. Because the ETC is small enough for the relaxation to be neglected (i.e., the duration of atomic flights does not allow for relaxation processes to occur), one simply gets

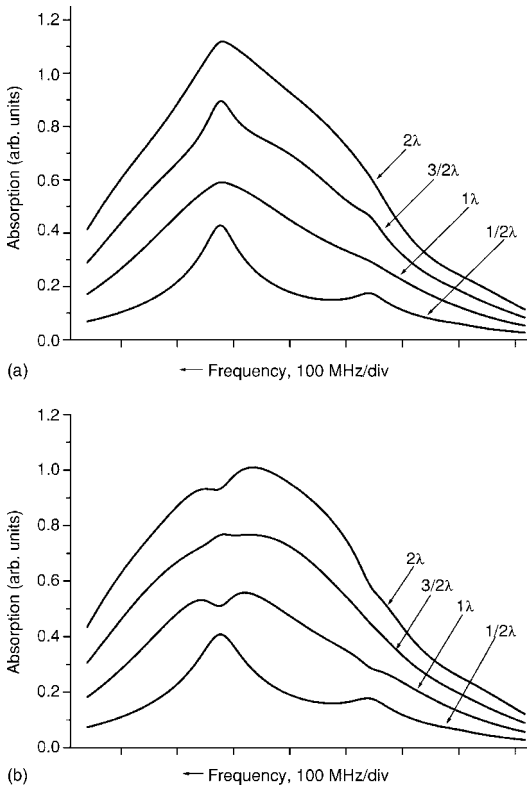

FIG. 3. The results of the numerical simulations of the absorption spectra depending on the value $L/\lambda=0.5$; 1; 1.5; 2, for laser linewidth $\Gamma_L\sim 3.5\gamma$. The Rabi frequency of the coupling laser field is $\Omega=0.2\gamma$ (a) and 1.5γ (b).

$$d\mathbf{S}/dt=\mathbf{S}\times\mathbf{B}. \tag{1}$$

For a given velocity group, $\mathbf{B}$ is constant so that the Bloch vector $\mathbf{S}$ describes a cone (see Fig. 5), traveled at a constant angular velocity $\Delta=\sqrt{(\Omega^2+\delta^2)}$ proportional to B, and tangent to the initial Bloch vector $\mathbf{S}_0=(0,0,-1)$ (note that S_z is the population inversion). The evaluation of the optical properties of the ETC requires a spatial integration in the ETC of the local values of $\mathbf{S}(z)$ that is calculated through its transient evolution on a duration $t=z/v_\perp$ ($v_\perp$ is the velocity component normal to the ETC windows) for $v_\perp>0$, or $t=z'/v_\perp$ for $v_\perp<0$ ($z'\equiv L-z$). The absorption and fluorescence in the ETC hence appear, respectively, governed by $\int_0^L S_y(t=z/v_\perp)dz$, and $\int_0^L[1+S_z(t=z/v_\perp)]dz$ (for simplicity, the Fabry-Perot nature of the ETC [11] is neglected here). For a nonsaturating irradiation (e.g., $\Omega\ll\delta$), and close enough to resonance, the actual detuning $\delta-kv_\perp$ is sensitively equal to the Doppler-shift itself $-kv_\perp$ (i.e., $|\delta|\ll k|v_\perp|$), so that the $\mathbf{S}$ vector rotates at an angular velocity nearly proportional to $v_\perp$, but for a duration inversely proportional to $|v_\perp|$. This means that for all positive velocities, the angle described by the Bloch vector around the cone axis is $-kz$ (or kz' for all negative velocities). In consequence, the spatial integration is performed on an identical angular fraction $kL/2\pi=L/\lambda$ of the cone (whose half-angle is inversely proportional to $|v_\perp|$).

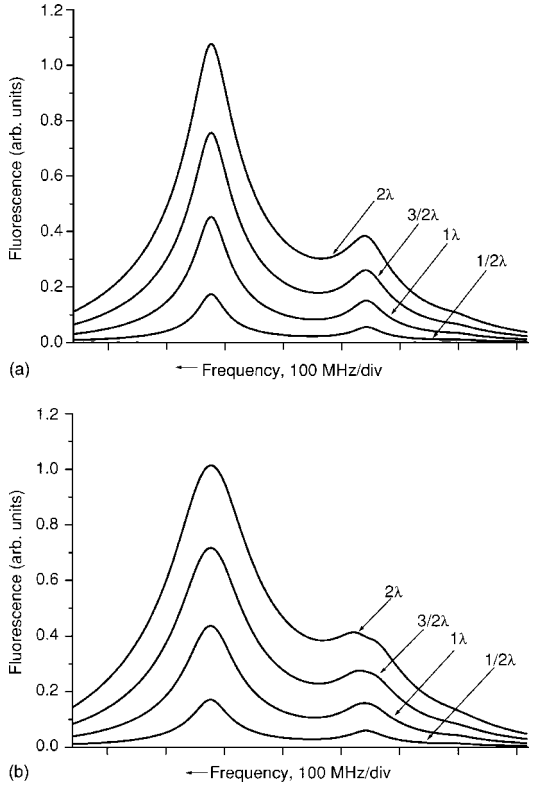

FIG. 4. The results of the numerical simulations of the resonant fluorescence spectra depending on the value $L/\lambda=0.5$; 1; 1.5; 2 for laser linewidth $\Gamma_L \sim 3.5\gamma$. The Rabi frequency of the coupling laser field is $\Omega=0.2\gamma$ (a) and 1.5γ (b).

Noting that the initial conditions for **S** impose that S_y oscillates around a null value, while $(1+S_z)$ oscillates from zero to a positive value, one understands that for $\delta \approx 0$ the absorption reaches a maximum for $L=\lambda/2$ and returns back to zero for $L=\lambda$, while the fluorescence grows continuously with the cell length. This result, obtained in the limit of a negligible relaxation, can be seen as an elementary signature of the coherent Dicke narrowing that affects the absorption and not the fluorescence. It can be added that, for an off-resonance irradiation, the speed of rotation depends both on δ and on $kv_\perp$, washing out the oscillating behavior predicted in absorption between $L=\lambda/2$ and $L=\lambda$, justifying the narrow spectral signature when the ETC length is around $\lambda/2$.

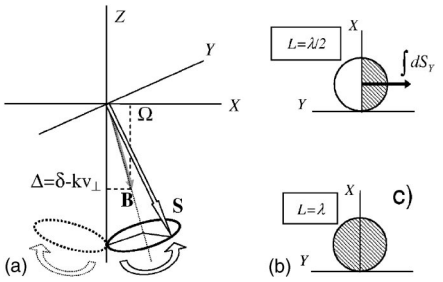

FIG. 5. (a) The figure shows the Bloch vector **S**. The full circle describes the trajectory followed by the tip of the **S** vector over time for positive velocity. The dotted circle stands for the trajectory described for a negative velocity $v_\perp$ implying that the **S** vector rotates in the opposite direction. (b) Projection on the *XY* plane of the Bloch vector trajectory for a given velocity class ($kv_\perp \gg |\delta|, \Omega$). The shaded area shows the angular sector contributing to $\int_0^L S_y(z)dz$ for a cell of length $L=\lambda/2$; (c) Same as (b) for $L=\lambda$.

To summarize, the fluorescence and absorption spectra of the Rb D_2 line have been studied with the help of a unique ETC with smoothly controllable thickness of atomic vapor layer, in the range $\sim 150-1800$ nm, for which the ETC thickness L is smaller or comparable to λ. Under all experimental conditions, the resonant fluorescence yields a narrower signal than the direct transmission signal, with an optimal value always obtained around $L=\lambda/2$. This optimum, sharply obtained at $L=\lambda/2$ for transmission, is followed by an oscillating linewidth behavior typical of the coherent Dicke narrowing. Conversely, the fluorescence behavior evolves much more smoothly with the cell length L, the observed broadening being simply attributed to a less stringent velocity selection.

This work was partly supported by the Armenian Ministry of Economics, Grants No. 02-1351 and No. 02-1323. The French-Armenian cooperation receives special support from University Paris13 and from CNRS, and the French-Uruguayan cooperation is supported by ECOS-Sud (U00-E03).

[1] S. Briaudeau, D. Bloch, and M. Ducloy, Europhys. Lett. **35**, 337 (1996).
[2] S. Briaudeau *et al.*, Phys. Rev. A **57**, R3169 (1998).
[3] S. Briaudeau *et al.*, Phys. Rev. A **59**, 3723 (1999).
[4] S. Briaudeau *et al.*, J. Phys. IV **10**, Pr8-145 (2000).
[5] A. Izmailov, Laser Phys. **2**, 76 (1992); Opt. Spectrosc. **74**, 25 (1993).
[6] T. A. Vartanyan and D. L. Lin, Phys. Rev. A **51**, 1959 (1995).
[7] B. Zambon and G. Nienhuis, Opt. Commun. **143**, 308 (1997).
[8] D. Sarkisyan *et al.*, Opt. Commun. **200**, 201 (2001).
[9] G. Dutier A. Yarovitski, S. Saltiel, A. Papoyan, D. Sarkisyan, D. Bloch, and M. Ducloy, Europhys. Lett. **63**, 35 (2003).
[10] R. H. Romer and R. H. Dicke, Phys. Rev. **99**, 532 (1955).
[11] G. Dutier *et al.*, J. Opt. Soc. Am. B **20**, 793 (2003).
[12] G. Dutier *et al.*, J. Phys. IV **12**, Pr5, 155 (2002).
[13] D. Sarkisyan *et al.*, CLEO/QELS-2003, Baltimore, QThJ 12 (2003).
[14] As the laser hits an ETC region of fairly good flatness, the overall observed fluorescence, which may partly originate from the vicinity of the irradiated region, actually comes from a region whose thickness must be considered as well-defined.
[15] D. Sarkisyan *et al.*, Appl. Phys. B: Lasers Opt. **76**, 625 (2003).
[16] D. Sarkisyan *et al.*, Opt. Spectrosc. (to be published).